Detection of Simultaneous Mechanical Faults in 6 kV Pumping Induction Motors Using Combined MCSA and Stray Flux Methods

Detection of Simultaneous Mechanical Faults in 6 kV Pumping Induction Motors Using Combined MCSA and Stray Flux Methods

Konstantinos N. Gyftakis [1*], Panagiotis A. Panagiotou [2], Dimitrios Spyrakis [3]

[1] School of Engineering, University of Edinburgh, The King's Buildings, Edinburgh, EH93DW UK
[2] Institute for Future Transport and Cities, Coventry University, 3 Gulson Rd, Coventry CV1 2JH, UK
[3] Public Power Corporation, Generation Division, Pigai Aoos Hydro Plant, Greece
[*] k.n.gyftakis@ieee.org

Abstract: The popularity of stray and air-gap flux monitoring methods is increasing. This trend is justified by several advantages of such methods over the stator current monitoring that has been demonstrated for electrical faults detection in induction and synchronous machines. However, the use of the magnetic flux for mechanical faults detections has not drawn this much attention while in industry the vibration analysis continuous to be popular. This paper comes to bridge this gap via the detection of mechanical faults of 6 kV induction motors in a pumping station. The diagnostic procedure mainly involves the stator current and stray flux monitoring and harmonic index analysis. The localisation of the fault has been made possible via oscillometer readings. It will be shown that mechanical faults have very different impact on the stator current and the flux signals, while the flux is not sensitive to the bearing fault mechanisms.

1. Introduction

Electrical machines are the heart of the modern world producing electric power or consuming it to produce mechanical work and consequently products and services. Due to their critical role for our sustainability, electrical machines condition monitoring and fault diagnosis has known a significant advancement. This is because undetected faults will evolve into higher severity levels and lead to catastrophic machine failures with a series of negative persecutions such as high financial losses, production delays and compromisation of safety [1]-[4].

Surveys and reviews have shown that the failure modes are dependent on the size of the electrical machines [5]-[7]. Low voltage motors suffer mainly from mechanical faults which consist three quarters of total faults. Medium voltage motors are quite interesting because bearing faults are the dominant fault but with very low difference than stator faults. However, the use of sleeve bearings in large machines consist stator faults the most frequent faulty condition. The various faults frequency is shown in Fig. 1 as a function of the size of the electric motor.

Various methods have been developed over the years aiming for the detection of different faults in induction motors. The favourite seems to be the MCSA (Motor Current Signature Analysis) [8]-[11]. The application of this method depends on the monitoring of the motor's current during operation and the analysis of its frequency spectrum via the FFT (Fast Fourier Transform). Despite its acceptance from industry, this method has been found unreliable in late years leading to false alarms due to various conditions of induction machines [12]-[14].

Other diagnostic methods include the use of the motor's output torque [15]-[16], vibrations monitoring [17]-[18], stray flux [19]-[21] and input electric power [22]-[23]. Among those, the stray magnetic flux appears to be quite promising due to the associated low-cost and non-intrusive character while it has proved to be immune to certain phenomena leading to false alarms with the MCSA [24]. The stray flux monitoring allows the capture and analysis of either the axial flux or the radial one or a combination of both depending on the positioning of the flux sensors on the machine body (Fig. 2) [25]. The electromotive force sensed with the flux sensors is machine geometry free thus senses harmonics which are cancelled out or hidden in the stator current because it depends on the machine's number of poles.

This paper demonstrates the application of a series of diagnostic methods to detect and locate mechanical faults, such as bearing faults and misalignment, in 6 kV induction motors used for water pumping applications. No prior

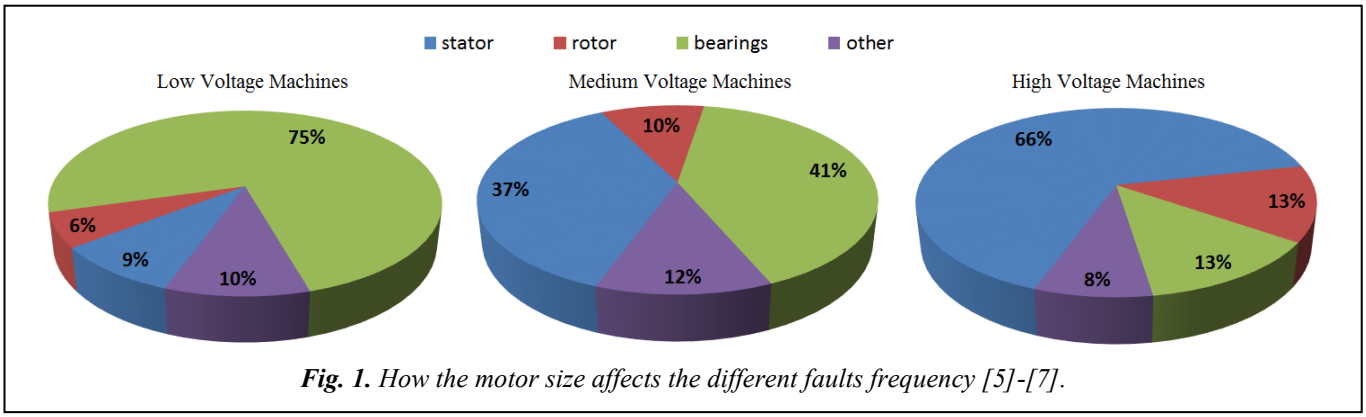

Fig. 1. *How the motor size affects the different faults frequency [5]-[7].*

knowledge of the mechanical system parameters existed. The work has been carried out with the simultaneous application of the MCSA and flux monitoring, while the localisation of the fault has been achieved by the supplementary use of an oscillometer. The results demonstrate that the stray flux is not sensitive to actual bearing faults, while the stator current is there superior. However, the stray flux monitoring seems sensitive to the misalignment fault and consequent mechanical oscillations. However, since in electrical faults monitoring, the stator current is not always reliable, thus for generalised monitoring it is necessary for the two methods to work together but focusing on different failures [26]. A detailed discussion will close this paper.

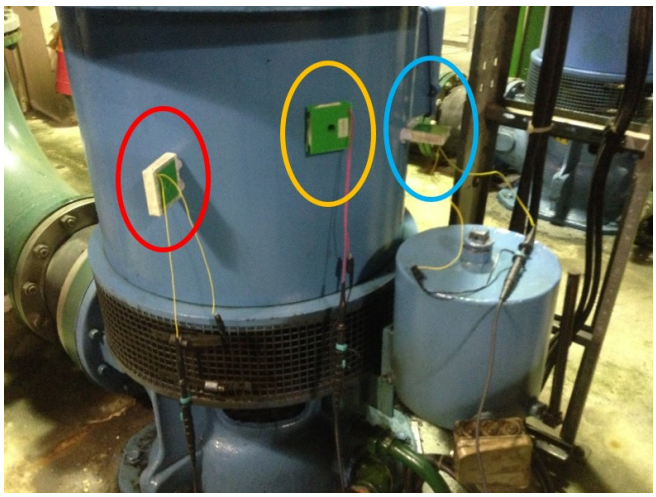

Fig. 2. *Radial (red), axial (blue) and combination of both (orange) stray flux monitoring.*

2. The Pumping Systems' Operating Characteristics

The primary aim of the monitored system is to pump water from the torrent to the main lake of the hydro plant. The water is pumped up to 20 m. To serve this purpose, 5 vertically installed motors driving pumps are used. During the visit, one of the motors (Motor 1) was stopped due to pump repairs and thus has not been considered in this study. The monitored 4 motors' nameplate data are presented in the following Tables 1 and 2. Furthermore, the motors as well as their associated pumps are illustrated in the following Fig. 3 and Fig. 4.

Three out of those five pumping systems are identical with a supply of 2 m^3/s, manometric 20 m and power 750 kW. The rest two pumping systems are smaller with a supply of 0.75 m^3/s, manometric 20 m and power 240 kW. All five pumps have a shaft which is 15 m long which rotates with the help of 6 grease bearings.

Table 1 Nominal Characteristics of Motors 3 and 5

Speed (rpm)	Power (kW)	cosφ	Voltage (V)	Current (A)	Frequency (Hz)
745	750	0.83	6000	71	50

Table 2 Nominal Characteristics of Motors 2 and 4

Speed (rpm)	Power (kW)	cosφ	Voltage (V)	Current (A)	Frequency (Hz)
990	240	0.82	6000	30.5	50

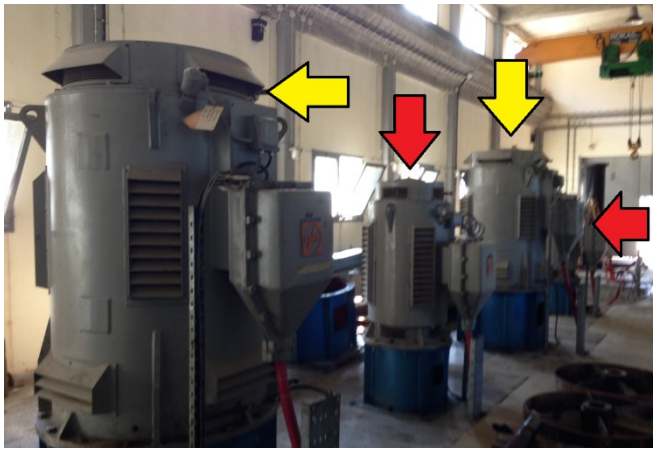

Fig. 3. *The vertically installed induction motors of 750 kW (yellow arrows) and 240 kW (red arrows).*

Fig. 4. *The associated pumps located at the lower level, 15 m below.*

3. Monitoring of Electromagnetic Signals

The four motors were operating under rated conditions when the condition monitoring took place. More specifically, current clamps were installed to each motor's supply to capture the stator current waveforms (Fig. 5). At the same time, flux sensors were placed on the motors' bodies. Aiming to detect possible faults with axial impact, such as a possible level of inclined eccentricity or a bent shaft, two flux sensors were installed on each motor perfectly aligned and in parallel with the motor shaft. Their surface is perpendicular to the radial direction, thus they monitor a combination between axial and radial flux. However, due to their long distance from the ends of the machine, the main dominant contributor is the radial flux component. The installed flux sensors on one of the motors are illustrated in the following Fig. 6.

The stator current measurements were carried out without an MCSA commercial equipment. Current clamps were used with a sensitivity of 10 mV/A and an accuracy of ±1% of reading at ±100/±500 mA. Providing a safety BNC connector, this measurement was at later stage logged onto a digital high resolution buffer memory unit used for acquisition of signal waveforms and data. All three stator currents were recorded for 3-phase inspection and detection of possible asymmetries.

There are two options for monitoring the stray flux namely the rigid coil sensors and Hall sensors. In this case, coil sensors have been applied. The sensors were built in the lab using a custom made winding machine and a 3D printer. The sensors geometrical features are shown in Fig. 7.

Due to the high reluctance of the air, the stray flux is generally weak. This is why, the flux sensors were designed under two constraints: low coil length and high number of turns. The coil was built with a very fine copper wire of 0.1 mm diameter leading to a total of 3500 turns. The per-length resistance of the wire is 3.4 Ω/m. During operation the rotating magnetic field will induce an electromotive force to the sensors, so in order to record that, a voltage probe was installed at every sensor recording the voltage across the coil turns.

The current and flux sensor signals are captured by a portable high resolution, deep memory, 8-channel oscilloscope. Offering a 12-bit resolution and serial bus decoding with 256 MS buffer memory and a 20 MHz bandwidth, each signal waveform was captured within 12 frames of 10 sec each, providing the ability to gather extended waveforms over the steady state of the motors for reliable signal representation in both the time and frequency domain. The sampling frequency has been 15 kHz.

Fig. 5. *Installation of the current sensors at the terminals of the induction motor.*

Fig. 6. *Installation of the flux sensors in parallel to the motor shaft.*

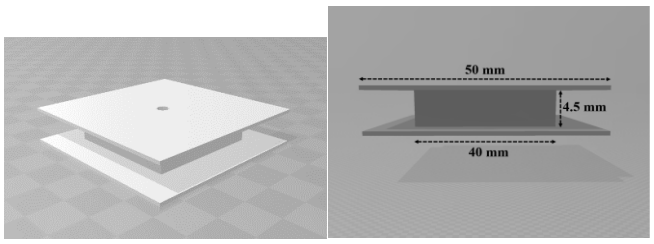

Fig. 7. *The flux sensors body dimensions.*

4. Stator Current Monitoring

Due to lack of past history and healthy condition data, the stator current spectra are compared between identical motors of the same power. The MCSA results for Motors 3 and 5 are shown in the following Fig. 8.

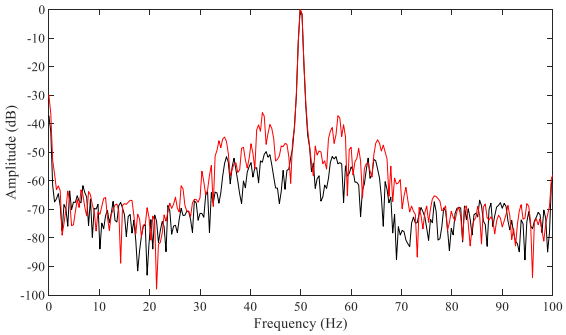

Fig. 8. *Comparative MCSA specta of Motors 3 (black) and 5 (red) while at steady state.*

The stator current spectra analysis reveals the existence of additional harmonics in Motor 5. The harmonics appear as sidebands of the fundamental harmonic at 50 Hz. The first local maximum is located at 42.38 Hz, that is: $f_s - f_o$, $f_o = 7.62$ Hz. However the right sidebands appears as well together with multiples of this frequency. The recorded amplitudes of the $f_s \pm k \cdot f_o$ sidebands are shown in Table 3.

Interestingly, extra sidebands appear next to each one of the above mentioned harmonics. The right one has distance

Table 3 MCSA harmonics and amplitudes (dB)

frequency	fs-2fo	fs-fo	fs+fo	fs+2fo
Motor 3	-50.51	-49.79	-51.52	-50.95
Motor 5	-44.67	-36.12	-37.21	-45.62

Table 4 Harmonics in Motor 5 (Hz)

fs-2fo	fs-fo-for	fs-fo	fs-fo+for
34.76	41.30	42.38	43.88
fs+fo-for	fs+fo	fs+fo+for	fs+2fo
56.54	57.62	59.12	65.24

f_{or} =1.5 Hz, while the left f_{ol} =1.08 Hz from the $f_s \pm k \cdot f_o$ ones. The amplitudes of all sidebands are summarised in Table 4.

The observed fault harmonics in Motor 5 do not obey to the well-known formulas revealing rotor eccentricity (f_{ecc}) [4] or broken rotor bar/end ring failures (f_{bb}) [27], as shown below:

$$f_{ecc} = \begin{cases} f_s \pm k\frac{(1-s)f_s}{p} \\ \left[(R \pm n_d)\left(\frac{(1-s)}{p}\right) \pm 2n_{sa} \pm n_{ws}\right] f_s \end{cases} \quad (1)$$

$$f_{bb} = \left[\frac{k}{p}(1-s) \pm s\right] f_s\,, \quad (2)$$

where $k = 1,2,3,\ldots, R$: the rotor slot number, s: the slip, p: the number of pole pairs, f_s: the fundamental frequency, $n_d = 0\,(for\ static), 1, 2, 3, \ldots (for\ dynamic)$, n_{sa}: the saturation effect (=1, 2, 3,…) and n_{ws}: time harmonic rank (=1, 2, 3,…).

It is to be noted that, the first part of (1) is for mixed eccentricity while the second for only-static, only-dynamic or a combination of both.

Since the observed signatures are not satisfied by either equations (1) or (2), they should be caused by some mechanical failure. Bearing faults is the first that comes to mind. Rolling element bearing faults cause signatures at frequencies [4], [28]:

$$f_{bearings} = f_s \pm m \cdot f_{i,o,c} \quad (3)$$

where m=1,2,3,… and $f_{i,o}$ and f_c given by:

$$f_{i,o} = \frac{N_b}{2} f_r \left(1 \pm \frac{D_b}{D_c}\cos\beta\right) \quad (4)$$

$$f_c = \frac{f_r}{2}\left(1 - \frac{D_b}{D_c}\cos\beta\right) \quad (5)$$

where N_b, f_r, D_b, D_c and β are the number of bearing balls, the mechanical rotor speed frequency, the ball diameter, the bearing pitch diameter and the contact angle of the balls respectively. The frequency subscripts i, o, c stand for the ball pass inner raceway, the ball pass outer raceway and the fundamental cage.

As a rule of thumb and if the number of balls in between six and twelve, the corresponding values can be calculated as follows:

$$\begin{cases} f_o = 0.4 N_b f_r \\ f_i = 0.6 N_b f_r \\ f_c = 0.4 f_r \end{cases} \quad (6)$$

5. Magnetic Flux Monitoring

As mentioned before, two sensors have been installed on every induction motor and they monitor a combination of axial and radial flux. The EMF waveforms have been analysed with the application of the FFT and their frequency spectra are presented in the following Fig. 9-10.

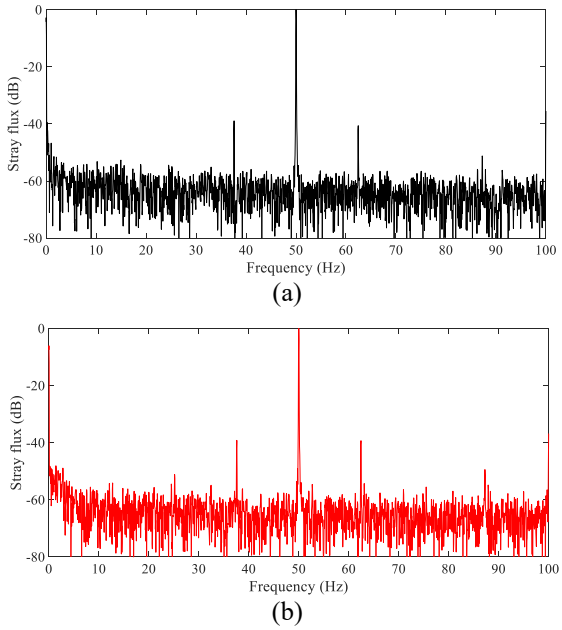

Fig. 9. *FFT spectra of the sensor EMF of: (a) low and (b) high positioned sensors of Motor 3 at steady state.*

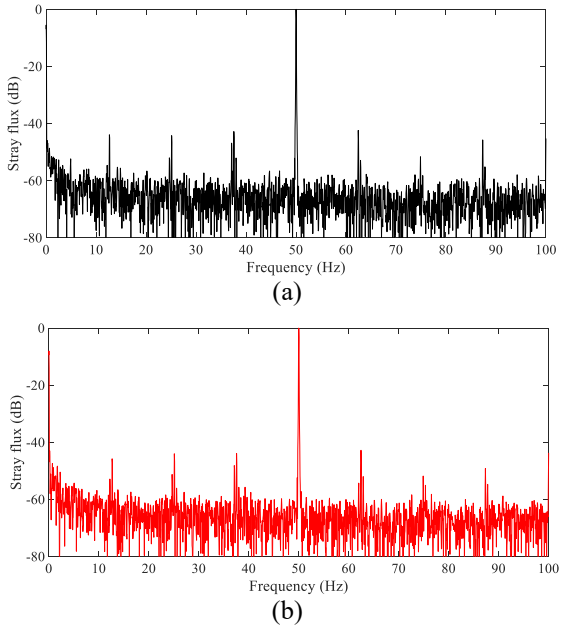

Fig. 10. *FFT spectra of the sensor EMF of: (a) low and (b) high positioned sensors of Motor 5 at steady state.*

From Figs 9-10, no axial dissymmetry is detected in both motors as the spectra from both sensors are almost identical. This is further supported by the flux waveforms over time such as the one for Motor 5 shown in Fig. 11, where one can see that the two sensors top and bottom monitor almost perfectly identical flux signals. Furthermore, it becomes evident that the observed stator current harmonic sidebands of Motor 5 are completely absent in the flux. Despite that, Motor 5 is characterised by increased harmonic index at frequencies associated with the mechanical speed: $f_r = \frac{(1-s)}{p} f_s$. More specifically, both sensors mounted on Motor 5 have captured harmonic components at frequencies: $f_s \pm k \cdot f_r, k \in \mathbb{N}$. This signatures series exists very clearly for values: $k = [-3, 3]$. On the other hand, Motor 3 has only

the main sidebands for $k = [-1, 1]$. These harmonics are well known to be associated with mixed eccentricity [29] and misalignment [30] conditions, however it is worth mentioning that they have been lately associated to rotor electrical faults as well [31]. However, no signs of rotor electrical faults exist in the stator current, a fact that leads to the eccentricity or misallignment as the main suspect for producing the above harmonics in the flux. The frequency f_r has been found to be 12.45 Hz, which is synonymous to a mechanical speed 747 rpm. The amplitudes of all eccentricity harmonics have been extracted and presented in the following Tables 5 and 6. The increased harmonic index om Motor 5, associated with mixed eccentricity and load imbalances, supplements the harmonic index of the stator current that points towards bearing failures while these two conditions are always related and often appear together. Interestingly, the mechanical frequency related harmonics do not clearly appear in the stator current, possibly due to low oscillations level.

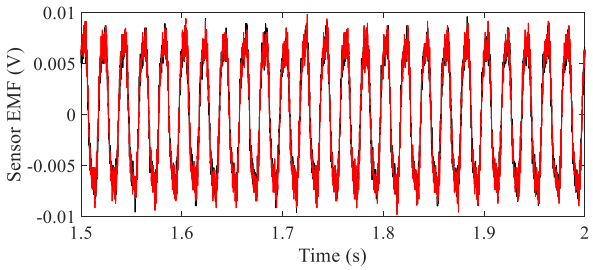

Fig. 11. *Recorded flux sensor signals over time of Motor 5 where top sensor in black and bottom in red.*

Table 5 Motor 3 Flux Eccentricity Signatures (dB)

position	fs-3fr	fs-2fr	fs-fr	fs+fr	fs+2fr	fs+3fr
low			-38.94	-40.64		-51.21
high		-51.14	-39.18	-39.3		-49.41

Table 6 Motor 5 Flux Eccentricity Signatures (dB)

position	fs-3fr	fs-2fr	fs-fr	fs+fr	fs+2fr	fs+3fr
low	-43.95	-44.25	-42.8	-42.41	-51.64	-45.74
high	-45.78	-44.02	-43.9	-42.79	-51.82	-49.19

6. Additional Investigation and Diagnostic Analysis

The mechanical system's properties are unknown while involving many different bearing types namely: motor bearings, shaft bearings and pump bearings. In any case, the multiple harmonics of the current spectra indicate a complex failure. Absent geometrical data, equation 6 is applied while taking into account that the mechanical frequency is 12.45 Hz. For $6 < N_b < 12$, equation 6 gives:

$$\begin{cases} 29.88\ Hz \le f_o \le 59.76\ Hz \\ 44.82\ Hz \le f_i \le 89.64\ Hz \\ f_c = 4.98 \end{cases} \quad (7)$$

The harmonics described by (7) need to be subtracted from the fundamental in order to point at possible fault signatures in the stator current spectrum (eq. (3)). Table 7 summarizes all the possible signatures' locations.

The signatures that look to be close to the ones monitored in the MCSA spectrum appear in bold. Of course this is just an indication and not proof because the harmonics have been calculated by approximated formulae. In any case, inner raceway and cage faults may produce the observed stator current harmonics. As a result, and since broken rotor bars or other rotor electrical failures have been excluded as possible, the diagnostic conclusion is that the fault is of mechanical nature and most probably a combination of different faults.

The source of the fault is still unknown though. In such systems with a long distance between motor and pump it is of interest to locate the fault with accuracy as this would save a lot of money and time for the inspection and repair. In order to pinpoint the exact source of the main failure, a supplementary diagnostic step was taken. Extra measurements were taken using a portable oscillometer with the following characteristics:

(parameters are specified at 25°C)

- Sensitivity: 20mV/mm/s ±5% at 100Hz
- Sensitivity Temperature Coefficient: 0.2%/°C
- Frequency response: 4.5Hz to 1000Hz + 0, -3dB

The use of the oscillometer at the induction motor's load side is presented in Fig. 12. Detailed recordings were taken at the motor and the pump sides.

The oscillation measurements were as follows at the different points of interest:

- Upper motor part (x-axis *35 μm* p-p, y-axis at direction of the discharge tube *27 μm* p-p).
- Lower motor part (x-axis *18 μm* p-p, y-axis at direction of discharge tube *20 μm* p-p).
- Middle pump part (x-axis *120 μm* p-p, y-axis at direction of discharge tube *110 μm* p-p).
- Lower pump part (x-axis *72 μm* p-p, y-axis at direction of discharge tube *70 μm* p-p , z-axis 70 μm p-p).

Table 7 Estimated Bearing Fault Signatures (Hz)

balls	6	7	8	9	10	11	12
|fs-fo|	20.12	15.14	10.16	5.18	0.2	4.78	9.76
|fs-fi|	5.18	2.29	9.76	17.23	24.7	32.17	**39.64**
|fs-fc|	**45.02**	**45.02**	**45.02**	**45.02**	**45.02**	**45.02**	**45.02**
|fs+fc|	**54.98**	**54.98**	**54.98**	**54.98**	**54.98**	**54.98**	**54.98**

Fig. 12. *Displacement measurements with the oscillometer at the load side of Motor 5.*

The additional investigation using the oscillometer lead to the conclusion that increased oscillations appeared at the middle and lower part of the pump. The diagnostic outcome from the motor's behaviour led to the conclusion that the observed electromagnetic index was due to shaft misalignment causing faster ageing of the bearings and possible impeller damage. Therefore, the shaft had to be dismantled (Fig. 13) and the impeller replaced. The inspection showed extensive degradation of all of them.

Fig. 13. *The dismantled shaft.*

A degradation of the load part with such degradation severity level was improbable to have left the motor completely intact. That logical conclusion however was not supported by the measurements. On one hand, the MCSA analysis did not reveal any important eccentricity harmonics in the stator current, while on the other the oscillometer readings were quite low and non-alarming. Despite that, since the system was not operational due to the load repair, a decision was made to inspect the induction motor as well. The inspection also revealed that the misalignment had actually caused significant damage at the induction motor's bearings, which also had to be replaced (Fig. 14). The damage was distributed in a uniform manner along the circumference of the bearings. Interestingly though, the degradation had affected the bearings in the axial direction and not the radial, possibly due to axial oscillations. It has been concluded that, the vertical alignment of the installation together the uniform degradation of the motor's bearings were probably shielding the fault's existence from both diagnostic approaches applied in this work.

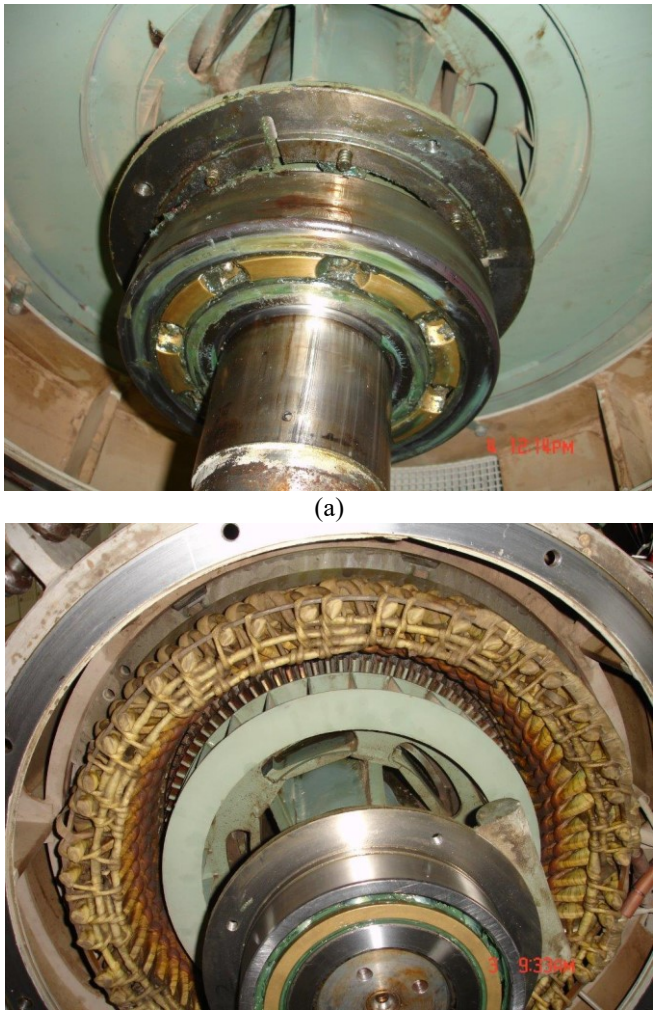

(a)

(b)

Fig. 14. *The motor without protective side covers: (a) before and b) after the bearings replacement.*

7. Critical Discussion

In this session an effort will be made to critically appraise the outcomes form this work with the literature and extract useful conclusions for future research efforts.

Firstly, this work clearly shows that the MCSA is highly sensitive to mechanical failures. The signatures were very clear and with significant amplitudes clearly leading to a diagnostic alarm. The method relies on the adoption of the induction motor itself and more specifically its stator winding as the sensor to depict failures in the whole system, in this case faults coming from the shaft bearings and the pump. There is superiority of the MCSA compared to vibration analysis associated with the low cost and remote monitoring capabilities.

Secondly, the stray flux is totally insensitive to the mechanical faults and consequent mechanical oscillations

that originate from the load. None of the signatures that appeared in the stator current spectrum existed in either of the two installed flux sensors. Despite that, the flux sensor was more sensitive to the rotor eccentricity and misalignment than the MCSA, leading to a family of many sidebands. Overall, the diagnostic contribution of the stray flux monitoring is this particular case was of low value.

Furthermore, when a system is considered, the diagnosis of the fault is the first necessary step. However, localisation of the fault is then required and to that purpose secondary methods are required (in this case the oscillometer measuring displacements and mechanical oscillations).

In recent literature, the stray flux appears to be the solution to many misdiagnosis cases associated with the MCSA such as the rotor axial cooling air ducts which are misinterpreted for broken rotor bars [24]. Past experience in the field strongly suggests that relying on the MCSA alone is not a reliable way to perform diagnostics. Furthermore, stator current based techniques proved insensitive to early stator inter-turn faults recently [32]. On the other hand, past works have also shown that the stray flux monitoring is insensitive to load defects [33]. This paper clearly indicates the incapability of bearing faults detection of the whole system (motor, shaft, pump) via the stray flux. The mechanisms that lead to this insensitivity should be quantified and understood in the future by more research and testing in the field in order to cover a statistically important population of electrical machines. However, the stray flux seems sensitive to the misalignment fault.

To summarise and while thinking about the current literature on diagnostics, it seems that one method alone cannot provide a full screening of the electrical machines' health. The combination of at least two methods will guarantee the reliability of the diagnosis, while the stray flux methods should replace MCSA on the electrical faults monitoring and MCSA is a good and advantageous replacement to the vibration analysis. Other secondary techniques such as oscillations here or thermography could localise the fault and add more information at a post-diagnostic and pre-service stage.

Finally, vertically mounted induction motors have a very different degradation mechanisms of their bearings compared to horizontally mounted ones and which are the majority. The geometrically uniform ageing of the bearing as well as the fact that the damages and cracks were formed in the axial and not radial direction led to this serious faulty case going completely undetected with conventional methods. In this paper, the oscillometer did not sense any important displacements or oscillations at the two motor ends. More research is required to fully understand how such failures can be reliably detected.

8. Conclusion

This paper has presented all the steps from the application of the MCSA and stray flux monitoring aiming to detect mechanical faults during a routine test in 6 kV induction motors driving pumps. At a time where the stray flux wins significant ground over the MCSA for electric faults detection, it becomes clear that it may be less sensitive to faults of mechanical nature and which are still detected via the stator current reliably. The paper has demonstrated a procedure to detect such faults without any prior knowledge of the geometrical and other features of the monitored system. Furthermore, a new challenge has been identified and concerns the detection and understanding of the underlying degradation mechanism of bearing faults in vertically mounted induction motors.

9. Acknowledgments

The authors gratefully acknowledge the contribution of Mr Evangelos Tirekoglou, Tech. Elec. Engineer and responsible ranking officer for the electrical maintenance of the hydro plant "Pigai Aoos", who technically supported the research team to collect the data.

10. References

[1] Ludeca Inc. Maintenance Study, 'Evaluating Energy Consumption on Misaligned Machines', 1994.
[2] Daintith, E., Glatt, P., 'Reduce Costs with Laser Shaft Alignment', Hydrocarbon Processing, August 1996.
[3] Trigeassou, J. C.: 'Electrical Machine Diagnosis', Wiley Press, ISTE, ISBN 978-1-84821-263-3, 2011.
[4] Toliyat, H. A. et al: 'Electric Machines: Modelling, Condition Monitoring, and Fault Diagnostics', CRC Press, ISBN 9781138073975, 2012.
[5] Seinsch, H. O.: 'Monitoring und Diagnose elektrischer Maschinen und Antriebe', in Proc. VDE Workshop, Allianz Schadensstatistik an HS Motoren, 1996–1999, 2001.
[6] Tavner, P. J.: "Review of condition monitoring of rotating electrical machines", IET Elec. Power Appl., 2008, 2 (4), pp. 215-247.
[7] Zhang, P. et al: 'A Survey of Condition Monitoring and Protection Methods for Medium-Voltage Induction Motors', IEEE Trans. Ind. Appl., 2011, 47 (1), pp. 34-46.
[8] Drakaki, M. et al 'Study on fault diagnosis of broken rotor bars in squirrel cage induction motors: a multi-agent system approach using intelligent classifiers', IET Elec. Pow. Appl., 2020, 14 (2), pp. 245-255.
[9] Pons-Llinares, J. et al: 'Mixed eccentricity diagnosis in Inverter-Fed Induction Motors via the Adaptive Slope Transform of transient stator currents', Elsevier MSSP, 2014, 48 (1-2), pp.423-435.
[10] Thomson, W. T., Culbert, I.: 'Motor Current Signature Analysis for Induction Motors, Current Signature Analysis for Condition Monitoring of Cage Induction Motors: Industrial Application and Case Histories', Book Chapter, John Wiley & Sons, Inc. Hoboken, 2016, pp. 1-37.
[11] Popaleny, P. et al: 'Electrical Submersible Pumps Condition Monitoring Using Motor Current Signature Analysis', In Abu Dhabi International Petroleum Exhibition & Conference, Society of Petroleum Engineers, Nov 2018.
[12] Concari, C., Franceschini, G. and Tassoni, C.: 'Differential Diagnosis Based on Multivariable Monitoring to Assess Induction Machine Rotor Conditions', IEEE Trans. Ind. Electr., 2008, 55 (12), pp.4156-4166.
[13] Lamim Filho, P.C.M., Pederiva, R. and Brito, J.N.: 'Detection of stator winding faults in induction machines using flux and vibration analysis', Elsevier MSSP, 2014, 42(1-2), pp.377-387.
[14] Gangsar P. and Tiwari, R.: 'Comparative investigation of vibration and current monitoring for prediction of

mechanical and electrical faults in induction motor based on multiclass-support vector machine algorithms', Elsevier MSSP, 2017, 94, pp. 464-481.
[15] Kia, S. H., Henao, H. and Capolino, G.A.: 'Torsonial vibration effects on induction machine current and torque signatures in gear-box based electromechanical system', IEEE Trans. Ind. Appl., 2009, 56 (11), pp. 4689-4699.
[16] Gyftakis, K. N. et al: 'Detection of Rotor Electrical Faults in Induction Motors during the Start-up via Torque Monitoring', IEEE IECON 2019, Lisbon, Portugal.
[17] Helmi, H. and Forouzantabar A.: 'Rolling bearing fault detection of electric motor using time domain and frequency domain features extraction and ANFIS', IET Elec. Pow. Appl., 2019, 13 (5), pp. 662-669.
[18] He G. et al: 'Frequency response model and mechanism for wind turbine planetary gear train vibration analysis', 2017, 11 (4), pp. 425-432.
[19] Zeng C. et al: 'Inter-turn fault diagnosis of permanent magnet synchronous machine based on tooth magnetic flux analysis', IET Elec. Pow. Appl., 2018, 12 (6), pp. 837-844.
[20] Panagiotou, P. A. et al: 'A New Approach for Broken Rotor Bar Detection in Induction Motors Using Frequency Extraction in Stray Flux Signals', IEEE Trans. Ind. Appl., 2019, 55 (4), pp. 3501-3511.
[21] Panagiotou, P. A. et al: 'FEM approach for diagnosis of induction machines' non-adjacent broken rotor bars by short-time Fourier transform spectrogram', IET The Journ. Of Engin., 2019, (17), pp. 4566-4570.
[22] J. Kim, J. et al: 'Power spectrum-based detection of induction motor rotor faults for immunity to false alarms', IEEE Trans. Ener. Conv., 2015, 30 (3), pp.1123-1132.
[23] Drif, M. H. et al: 'Active and Reactive Power Spectra-Based Detection and Separation of Rotor Faults and Low-Frequency Load Torque Oscillations', IEEE Trans. Ind. Appl., 2017, 53 (3), pp.2702-2710.
[24] Park, Y. et al: 'Stray Flux Monitoring for Reliable Detection of Rotor Faults under the Influence of Rotor Axial Air Ducts', IEEE Trans. Ind. Electr., 2019, 66 (10), pp. 7561-7570.
[25] Ceban, A., Pusca, R. and Romary, R.: 'Study of Rotor Faults in Induction Motors Using External Magnetic Field Analysis', IEEE Trans. Ind. Elec., 2012, 59 (5), pp. 2082-2093.
[26] Gyftakis, K. N., Panagiotou, P. A. and Spyrakis, D.: 'Recent Experiences with MCSA and Flux Condition Monitoring of Mechanical Faults in 6kV Induction Motors for Water Pumping Applications,, IEEE SDEMPED 2019.
[27] Riera-Guasp, M. et al: 'Diagnosis of induction motor faults via Gabor analysis of the current in transient regime', IEEE Trans. on Instr. & Measurement, 2012, 61 (6), pp.1583-1596.
[28] Faiz, J., Ghorbanian V. and Joksimovic, G.: 'Fault Diagnosis of Induction Motors', IET, 2017, pp. 104-105.
[29] Nandi, S. et al: 'Performance analysis of a three-phase induction motor under mixed eccentricity condition', International Conference on Power Electronic Drives and Energy Systems for Industrial Growth, 1998.
[30] Bossio, J. M., Bossio, G. R. and De Angelo, C. H.: 'Angular misalignment in induction motors with flexible coupling', 35th Annual Conference of IEEE Industrial Electronics, 2009, Porto, pp. 1033-1038.
[31] Gyftakis, K. N., Panagiotou, P. A. and Lee, S. B.: 'The Role of the Mechanical Speed Frequency on the Induction Motor Fault Detection via the Stray Flux', IEEE SDEMPED 2019.
[32] Gyftakis K. N. and Cardoso, A. J. M.: 'Reliable Detection of Stator Inter-Turn Faults of Very Low Severity Level in Induction Motors', IEEE Trans. Ind. Elec., 2020, early access.
[33] Park, Y. et al: 'Flux-based detection of non-adjacent rotor bar damage in squirrel cage induction motors', Proc. of IEEE ECCE, 2019, pp. 7019-7026.